Appl. Phys. B 84, 191–195 (2006)
DOI: 10.1007/s00340-006-2223-0

Applied Physics B
Lasers and Optics

H. WANG[1,4]
K. FU[2,4]
R.A. DREZEK[2,3,4]
N.J. HALAS[1,3,4,✉]

Light scattering from spherical plasmonic nanoantennas: effects of nanoscale roughness

[1] Department of Chemistry, Rice University, 6100 South Main Street, Houston, Texas 77005, USA
[2] Department of Bioengineering, Rice University, 6100 South Main Street, Houston, Texas 77005, USA
[3] Department of Electrical and Computer Engineering, Rice University, 6100 South Main Street, Houston, Texas 77005, USA
[4] Laboratory for Nanophotonics (LANP), Rice University, 6100 South Main Street, Houston, Texas 77005, USA

Received: 2 January 2006
Published online: 13 May 2006 •

ABSTRACT We have investigated the light scattering properties of smooth and roughened nanoshells with dipolar and quadrupolar plasmon resonances tuned to 830 nm. In the dipole resonant case small but measurable variations in the angle dependent light scattering (ADLS) due to the introduction of surface roughness are observed. In the quadrupole case, the distinctive side lobe scattering characteristic of quadrupolar emission is strongly quenched for roughened nanoshells.

PACS 81.07.-b; 78.67.-n

1 Introduction

The interaction of light with subwavelength structures is a topic of increasing interest and importance. Recent advances in clean room and chemical nanofabrication methods provide many opportunities to control both the geometry and composition of nanometer scale structures. These expanding capabilities allow us to broadly consider nanostructures as "nano-optical components" and to understand, in a more comprehensive manner, how optical frequency electromagnetic fields can be controlled and manipulated at nanoscale dimensions.

Surface plasmon waves supported by metals play a central role in subwavelength optics. Metallic nanostructures support localized plasmons with several important properties, such as resonance frequency, controlled by geometry. On resonance, incident light can be absorbed by the nanostructure or redirected as scattered light. Plasmon resonant nanostructures can therefore be thought of as optical frequency "nanoantennas", driven by an optical wave, which can redirect incident light into well-defined emission patterns in free space, or can couple light into nearby structures, such as thin films or waveguides.

We have previously shown that a specific nanostructure geometry consisting of a metallic shell of well-defined inner and outer radius, known as a nanoshell, supports a plasmon resonance whose frequency is sensitively controlled by the relative inner and outer dimensions of the shell [1–3]. Increasing the absolute size of the nanoshell increases the relative intensity of scattered versus absorbed light in its total optical extinction, allowing for the generation of scattered waves from dipolar and successively higher multipolar plasmons at distinct, well-defined wavelengths [4]. Thus both the core/shell ratio and the absolute size of the nanoshell provide important distinct parameters with which to control the scattering properties of the nanostructure at any given wavelength.

Recently we have begun to investigate how the introduction of nanoscale "texturing" or the presence of defects on the nanoparticle surface may affect the optical properties of metallic nanoshells [5]. There are several reasons for pursuing these studies. Surface roughness has long been known to relax the boundary conditions preventing the direct excitation of surface plasmon waves on macroscopic metal films [6], however, its role on a subwavelength structure where direct optical excitation is already possible has not yet been fully addressed. Experimentally realized nanoshells already have a small inherent degree of texturing or defects arising from the seeded growth method used to develop the spherical metallic shell layer on the surface of oxide nanoparticles. It is an interesting and important question whether or not the plasmon properties predicted by Mie scattering theory [2, 7–10] for analytically smooth nanoshells are significantly modified by surface roughness. One would anticipate that nanoparticles in the quasistatic limit should behave as perfect dipoles. However, the introduction of phase retardation effects and the excitation of higher order modes that result when overall particle size is increased may introduce more significant deviations from the case of a perfectly spherical particle in the dipole limit [11, 12]. This more mesoscopic regime is one of general interest in light scattering studies, due to the importance of scattering properties in applications such as bioimaging [13–19] In a more general sense, a wide variety of naturally occurring particles, such as biological structures [17–19] or atmospheric dust particles, are also known to have structured surfaces, yet the light scattering properties of such structures are not well studied.

We have recently reported a chemical method that can be used to increase texturing on Au nanoshells, providing a systematic experimental approach with which to study the effects of nanoscale surface roughness on light scattering from nanoparticles [5]. The plasmon resonant extinction spectra of textured nanoshells were compared with theoretical sim-

✉ Fax: +1-713-348-5686, E-mail: halas@rice.edu

ulations developed using a 3D finite-difference time domain method that accurately modeled the nonanalytical, highly textured nanoshell surfaces. Here it was seen that while the dipolar plasmon resonance extinction spectrum is robust with respect to surface roughness, the higher order plasmon resonances are significantly damped in the far field extinction spectrum with the onset of increasing nanoscale roughness, resulting in an overall redshifting of the nanoshell spectral envelope.

In this paper we examine the effects of nanoscale surface roughness on the light scattering properties of plasmon resonant Au nanoshells. We have examined the angular dependence of light scattering on resonance for both dipole and quadrupole resonant nanoparticles, and how this angular dependence varies with the introduction of surface roughness. In this case, the nanostructures must be fabricated such that the addition of texturing does not redshift the plasmon response of the nanostructures. This is accomplished by a chemical method which allows us to fabricate both smooth and textured plasmon resonant nanoparticles with the same far field spectral response. Using these tailored scatterers we were able to investigate the spatial distribution of resonant scattered light from nanoshells in two different geometries and sizes, selectively tuning the dipole and quadrupole resonances to the same laser wavelength. This approach allows one to suppress effects due to detuning of the plasmon resonance from the laser wavelength and to the material dispersion of Au in the wavelength region of interest in our light scattering measurements.

2 Surface roughening of Au nanoshells

The fabrication of rough nanoshells is schematically illustrated in Fig. 1a. Au nanoshells with relatively smooth surfaces were fabricated following a previously reported method [2]. Nanoscale roughness on the nanoshell surfaces was created by further deposition of metallic Au protrusions onto the surface of the smooth nanoshells. Ascorbic acid was used to reduce chloroauric acid ($HAuCl_4$) to metallic Au in the presence of cetyltrimethyl ammonium bromide (CTAB). It is known that CTAB and $HAuCl_4$ can form a Au(III)-CTAB complex, which can be reduced into Au(I)-CTAB complex by ascorbic acid. This Au(I)-CTAB complex can be further reduced to metallic Au upon introduction of Au nanoparticles as seed particles, an approach that has proven successful in the seed-mediated growth of Au nanorods [20–22]. In the present study, we use Au nanoshells as the seed particles, and nanoscale bumps are created on the surface of the nanoshells in the deposition processing. In the fabrication of Au nanorods, single-crystalline nanoparticles are used as the seed, which results in the formation of single-crystalline nanorods. In contrast, nanoshells possess multicrystalline surfaces created by growth and coalescence of a large number of ultrasmall, randomly oriented single crystalline domains [2, 5]. These tiny domains grow into nanoscale protrusions due to a slight variation in deposition with respect to domain orientation, thereby generating roughened surfaces on the nanoparticles. The as-fabricated rough nanoshells were washed twice by centrifugation and redispersion in water. The roughened nanoshells can be homogenously dispersed in water to form colloidal solutions.

The growth of bumps on the surface of nanoshells can be monitored by extinction spectroscopy over the time period of the chemical process. Figure 1b shows the evolution of extinction spectra of the nanoshells during the roughening process. In this set of experiments, we started from relatively smooth Au nanoshells with an average core radius of 93 nm and shell thickness of 12 nm (Fig. 3c). 10.0 μL of 1% $HAuCl_4$, 1.5 μL of 0.4 M ascorbic acid, and 90 μL of Au nanoshell solution ($\sim 6 \times 10^9$ particles mL^{-1}) were introduced into 1 mL 25 mM CTAB aqueous solution in sequence. Both the quadrupole and dipole plasmon peaks blueshift (due to the increasing

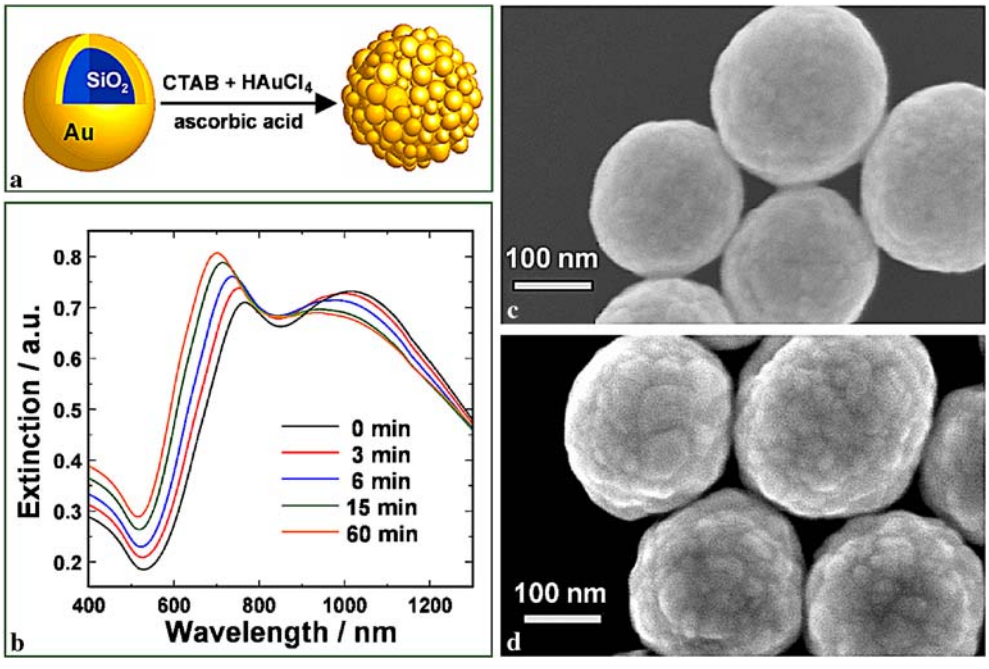

FIGURE 1 (**a**) Schematic illustration of the fabrication of rough nanoshells. (**b**) Evolution of extinction spectra of the nanoshells during the bump growth on the surface. SEM images of the nanoshells (**c**) prior to bump growth and (**d**) after bump growth for 60 min

thickness of the shell layer) and the quadrupole resonance significantly intensifies during the growth of the bumps. This indicates an increase in the thickness of the nanoshells [2]. As the bumps gradually grow larger, they may coalesce on the surface, leading to an increase in overall shell thickness in addition to bumpiness. The growth of bumps terminates after 60 min due to reactant depletion. As illustrated in Fig. 1d, the surface roughness of the nanoshells significantly increases with a large number of nanoscale bumps (15 to 50 nm in size) randomly arranged over the surface of the nanoparticles. By adjusting the ratio between the $HAuCl_4$ concentration, the density of the nanoshells in solution, and the thickness of the initial nanoshell layer, the surface plasmon resonance of the resulting roughened nanoshells can be systematically tuned. This provides a unique approach to selectively place dipole, quadrupole or even higher-order multipole plasmon resonances of roughened nanoshells at a wavelength of choice. In the case of this study, we tune the dipole and quadrupole plasmon resonances of the roughened nanoshells to the same wavelength as that of two corresponding sets of smooth nanoshells.

3 Tuning the plasmon resonance of the roughened nanoshells

In the present study, smooth nanoshells with suitable core radii and shell thicknesses were fabricated with dipole and quadrupole resonances at 830 nm, respectively. Mie scattering theory appropriate for a concentric core-shell geometry [7, 8] was used to calculate the optimal core-shell dimensions for smooth nanoshells. The quadrupole or dipole resonance of rough nanoshells was also carefully tuned to 830 nm by controlling the growth of bumps on the surface of smooth nanoshells. In Fig. 2a, dipole resonance of both smooth and roughened nanoshells are centered at ~ 830 nm, and a small shoulder at around 660 nm is also observed, corresponding to the quadrupole mode. In Fig. 2b, quadrupole resonances of smooth and roughened nanoshells are both tuned to 830 nm and the small shoulder at 680 nm is assigned to the octopole resonance. The dipole resonance peak is shifted into the infrared beyond the scanning range of the spectral measurements. The peak positions and lineshapes in the extinction spectra of the roughened nanoshells are very similar to those of the corresponding smooth nanoshells, except that a slight broadening of the plasmon peaks is observed for the roughened nanoshells. The broadening of the plasmon peaks is probably arising from the inhomogeneity of shell thickness caused by increased surface roughness.

4 ADLS measurements

A custom built ADLS apparatus was used in the present study (Fig. 3). The incident light source is a 30 mW GaAlAs diode laser with an output wavelength of 830 nm, and a Pico-Watt optical power meter (Model 1830-C, Newport) was used as the scattered light detector. The light is incident onto a cylindrical cuvette containing the nanoshell solutions through a linear polarizer, and the scattered light is collected by the power meter through another linear polarizer. The incident light is either horizontally or vertically polarized. The

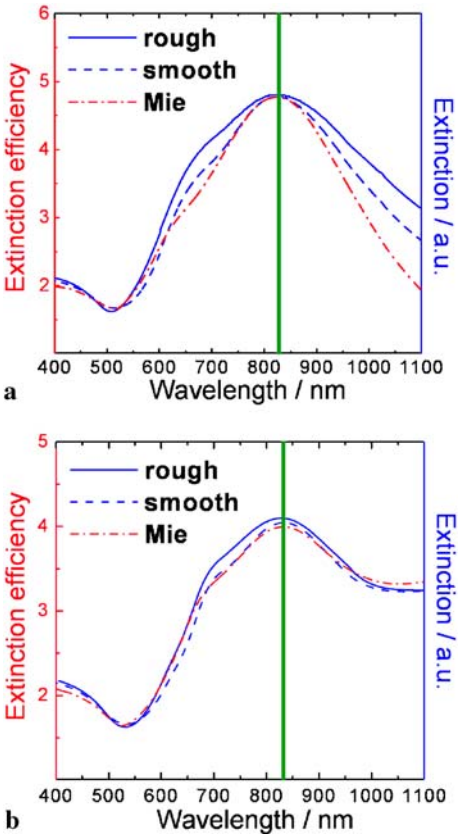

FIGURE 2 (**a**) Extinction spectra of smooth and roughened nanoshells (homogeneously dispersed in water) with dipole resonance at 830 nm. The smooth nanoshells have core radius of 65 ± 6 nm, and shell thickness of 14 ± 1 nm according to the SEM images. The *blue curves* are the measured spectra, and the *red dash-dotted curve* is the calculated curve according to Mie theory for a smooth nanoshell with 65 nm core radius and 14 nm shell thickness. The roughened nanoshells were fabricated by adding nanoscale bumps on the surface of smooth nanoshells with average core radius of 65 nm and shell thickness of 9 nm. (**b**) Extinction spectra of smooth and roughened nanoshells (homogeneously dispersed in water) with quadrupole resonance at 830 nm. The smooth nanoshells have a core radius of 148 ± 10 nm, and shell thickness of 20 ± 2 nm according to SEM images. The *red dash-dotted curve* is the calculated curve according to Mie theory for a smooth nanoshell with 150 nm core radius and 20 nm shell thickness. The roughened nanoshells were fabricated by adding bumps on the surface of smooth nanoshells with average core radius of 148 nm and shell thickness of 13 nm

horizontal polarization is defined as the light polarized in the same plane as the angle of detection is varied (parallel to the optical table) and the vertically polarized light is polarized perpendicularly to the table surface. The concentration of dipole resonant nanoshells is $\sim 2 \times 10^7$ particles mL^{-1} and that of the quadrupole nanoshells is $\sim 6 \times 10^6$ particles mL^{-1}. The light scattering data are collected in the range from 20° to 160°, with a step size of 1.8°.

The ADLS experiments were performed on dilute aqueous solutions of smooth and roughened nanoshells with dipole or quadrupole resonance at 830 nm whose extinction spectra are shown in Fig. 2. Figure 4 shows a direct comparison of the ADLS patterns of the smooth and roughened nanoshells illuminated at their dipole scattering resonance, plotted in polar coordinates. Mie theory is used to theoretically predict the angular distribution of light scattering from perfectly smooth nanoshells. Because the angular scattering distributions are spatially symmetric, only one side (scattering angle ranging

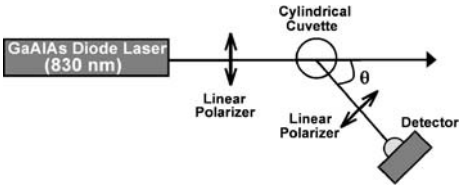

FIGURE 3 Components of the angle-dependent light scattering measurement apparatus

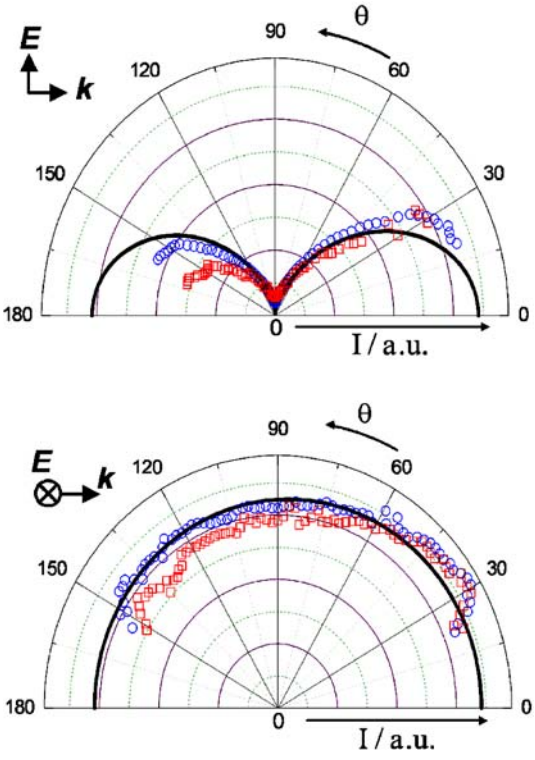

FIGURE 4 Angular dependent light scattering from smooth and roughened nanoshells excited at their dipole resonance with the (*top*) horizontally and (*bottom*) vertically polarized incident light. The light scattering patterns are plotted in polar coordinates. The *solid curves* are calculated curves for perfectly smooth nanoshells (65 nm core radius, 14 nm shell thickness) according to Mie scattering theory. The *blue circles* and *red squares* are the experimentally measured data for smooth and roughened nanoshells, respectively

from 0° to 180°) is measured. For both the horizontal and vertical polarizations, the experimentally measured ADLS patterns of the smooth nanoshells match Mie theory very well. The bimodal dipole scattering distribution applies for the horizontally polarized incident light, while the scattering curve is almost isotropic for the vertical polarization. For both polarizations, the introduction of nanoscale roughness on the surface of nanoshells does not lead to significant differences in their ADLS patterns in the forward scattering direction; however, a marked decrease in the light scattering intensities in the backward direction is observed for the rough nanoshell case.

In Fig. 5 we compare the ADLS patterns of the smooth and roughened nanoshells illuminated at their quadrupole resonances. The roughened nanoshells exhibit a significant deviation from Mie theory predictions for smooth nanoshells. Both the smooth and roughened nanoshells possess much stronger light scattering in the forward scattering direction than in the

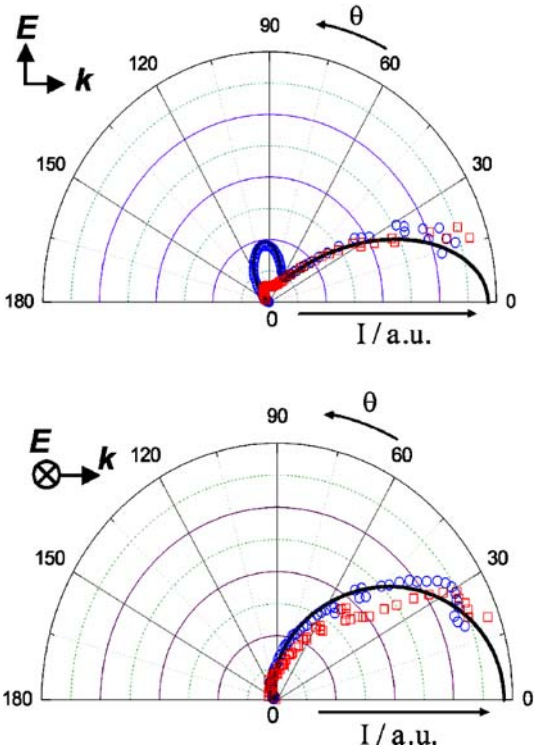

FIGURE 5 Angular dependent light scattering from smooth and roughened nanoshells excited at their quadrupole resonance with the (*top*) horizontally and (*bottom*) vertically polarized incident light. The *solid curves* are calculated curves for perfectly smooth nanoshells (150 nm core radius, 20 nm shell thickness) according to Mie scattering theory. The *blue circles* and *red squares* are the experimentally measured data for smooth and roughened nanoshells, respectively

backward direction. For smooth nanoshells, a secondary maximum at 95° is observed, in agreement with Mie theory, when the incident light is horizontally polarized. However, this side lobe completely disappears when nanoscale roughness is introduced on the surface of nanoshells. In the case of vertically polarized incident light, the roughened nanoshells present significantly weaker light scattering intensities in the range of 30°–100° than the corresponding smooth nanoshells.

5 Conclusions

In conclusion, roughened Au nanoshells have been fabricated by introducing nanoscale roughness on the surface of relatively smooth nanoshells. Both smooth and rough nanoshells were fabricated with dipole resonances and quadrupole resonances at the same laser wavelength of 830 nm. The effects of nanoscale surface roughness on the angular distribution of light scattering from these nanoshell antennas have been investigated both at the dipole and quadrupole resonances. Though the difference in far-field extinction spectra of the corresponding smooth and roughened nanoshells is minimal, the introduction of nanoscale roughness on the surface of nanoshells does result in measurable differences in the angular light scattering distributions. These observations may have important implications in the interpretation of light scattering characterization of complex nanostructures, and may lead to new ways of modifying the emission properties of resonant nanostructures.

ACKNOWLEDGEMENTS We would like to acknowledge the Air Force Office of Scientific Research (Grant F49620-03-C-0068), National Science Foundation (Grant EEC-0304097), National Aeronautics and Space Administration (NASA) (Grant 68371), the Robert A. Welch Foundation (Grants C-1220 and C-1222), Army Research Office (Grant DAAD19-99-1-0315), and Multidisciplinary University Research Initiative (MURI) (Grant W911NF-04-01-0203) for their financial support.

REFERENCES

1 R.D. Averitt, D. Sarkar, N.J. Halas, Phys. Rev. Lett. **78**, 4217 (1997)
2 S.J. Oldenburg, R.D. Averitt, S.L. Westcott, N.J. Halas, Chem. Phys. Lett. **288**, 243 (1998)
3 E. Prodan, C. Radloff, N.J. Halas, P. Nordlander, Science **302**, 419 (2003)
4 S.J. Oldenburg, G.D. Hale, J.B. Jackson, N.J. Halas, Appl. Phys. Lett. **75**, 1063 (1999)
5 H. Wang, G.P. Goodrich, F. Tam, C. Oubre, P. Nordlander, N.J. Halas, J. Phys. Chem. B **109**, 11 083 (2005)
6 H. Raether, *Surface Plasmons on Smooth and Rough Surfaces and on Gratings* (Springer, Berlin, 1988)
7 A.L. Aden, M. Kerker, J. Appl. Phys. **22**, 1242 (1951)
8 A.E. Neeves, M.H. Birnboim, J. Opt. Soc. Am. B **6**, 787 (1989)
9 J.B. Jackson, N.J. Halas, J. Phys. Chem. B **105**, 2743 (2001)
10 C. Nehl, N. Grady, G.P. Goodrich, F. Tam, N.J. Halas, J. Hafner, Nano Lett. **4**, 2355 (2004)
11 C.F. Bohren, D.R. Huffman, *Absorption and Scattering of Light by Small Particles* (Wiley, NY, 1998)
12 M. Kerker, *The Scattering of Light and Other Electromagnetic Radiation* (Academic, NY, 1969)
13 R.J. Cohen, G.B. Benedek, Immunochemistry **12**, 349 (1975)
14 J.R. Mourant, J.P. Freyer, A.H. Hielscher, A.A. Eick, D. Shen, T.M. Johnson, Appl. Opt. **37**, 3586 (1998)
15 J.R. Mourant, M. Canpolat, C. Brocker, O. Esponda-Ramos, T.M. Johnson, A. Matanock, K. Stetter, J.P. Freyer, J. Biomed. Opt. **5**, 131 (2000)
16 J.R. Mourant, T.M. Johnson, V. Doddi, J.P. Freyer, J. Biomed. Opt. **7**, 93 (2002)
17 R. Drezek, A. Dunn, R. Richards-Kortum, Appl. Opt. **38**, 3651 (1999)
18 R. Drezek, M. Guillaud, T. Collier, I. Boiko, A. Malpica, C. Macaulay, M. Follen, R. Richards-Kortum, J. Biomed. Opt. **8**, 7 (2003)
19 D. Arifler, M. Guillaud, A. Carraro, A. Malpica, M. Follen, R. Richards-Kortum, J. Biomed. Opt. **8**, 484 (2003)
20 B. Nikoobakht, M.A. El-Sayed, Chem. Mater. **15**, 1957 (2003)
21 B.D. Busbee, S.O. Obare, C.J. Murphy, Adv. Mater. **15**, 414 (2003)
22 A. Gole, C.J. Orendorff, C.J. Murphy, Langmuir **20**, 7117 (2004)